Wave Motion 87 (2019) 179–192

Contents lists available at ScienceDirect

Wave Motion

journal homepage: www.elsevier.com/locate/wamot

Geometrical theory of diffraction for sound radiation and structural response

A. Le Bot

Laboratoire de tribologie et dynamique des systèmes, UMR CNRS 5513, École centrale de Lyon, Université de Lyon, 36, av. Guy de Collongue 69134 Ecully, France

HIGHLIGHTS

- Application of geometrical theory of diffraction to fluid–structure interaction.
- Six types of structural/acoustical rays are identified.
- Explicit calculation of principal directions and curvature of wavefronts.
- Diffraction coefficients are given under light fluid assumption.

ARTICLE INFO

Article history:
Received 30 January 2018
Received in revised form 29 July 2018
Accepted 22 August 2018
Available online 23 August 2018

Keywords:
Geometrical acoustics
Rays
Diffraction
Sound radiation
Structural response

ABSTRACT

This study focuses on geometrical theory of diffraction (GTD) applied to vibroacoustics with a particular emphasis to fluid–structure interaction. Six types of hybrid rays are identified travelling either from structure-to-fluid (sound radiation) or from fluid-to-structure (structural response). Three rays correspond to sound radiation by the surface, edge, or corner of a structure while the three others are the reciprocal paths corresponding to sound-to-vibration conversion by the surface, edge, or corner. We present the calculation of geometrical properties of wavefronts (principal directions and curvatures) and their laws of transformation during an interaction process. Furthermore, some simple explicit relationships for diffraction coefficients are given under the light fluid assumption. Finally, two examples are discussed to illustrate the concepts. The first one is a pure radiation problem while the second one involves transmission through walls, structural response and sound radiation.

1. Introduction

The geometrical theory of diffraction (GTD) first developed by Keller [1,2] more than sixty years ago, is today a well-accepted and widespread method. This theory has many advantages to calculate wave fields in the presence of shadow zones. It has been widely employed in various fields of physics such as electromagnetics [3], acoustics, elastic waves [4,5]. In the field of acoustics, it has been applied to solve various problems, diffraction in inhomogeneous media [6], sound diffracted over wide barriers [7], rectangular box [8], sonic booms [9], multiple diffraction [10].

However, application of GTD to rays in mechanical structures is less common, probably because GTD best applies for exterior problems (typically diffraction by obstacles) where the number of rays reaching a point is finite or countably infinite. Most often, high frequencies in built-up structures are tackled by other methods based on boundary integral equations equivalent to ray-tracing without phase [11,12] or even by statistical energy analysis [13] when ray fields are diffuse.

E-mail address: alain.le-bot@ec-lyon.fr.

https://doi.org/10.1016/j.wavemoti.2018.08.009
0165-2125/

In bounded domains, GTD is generally implemented by ray-tracing like in room acoustics [14]. But in vibroacoustics, a further difficulty arises. Ray methods require to introduce simultaneously acoustical rays as well as structural rays. Since the conversion of a structural ray into acoustical ray (sound radiation) and conversely (structural response), may occur, we must admit the existence of hybrid rays.

Interaction processes between structural vibrations and acoustics are well-known. For instance, an overview of these processes described by means of a wave approach can be found in [15,16]. The problem of transmission of acoustical rays through finite plane plate using GTD including all diffraction effects is touched on in [17]. These authors identify four types of hybrid structural–acoustical rays associated with edge radiation and phase matched leakage of structure modes and their reciprocal rays. The coupling coefficients are not available in closed-form relationships but have been extracted from numerical simulations based on a fine resolution of governing equations.

The purpose of this study is to apply the geometrical theory of diffraction to sound radiation and structural response. GTD is here taken in its wider sense, that is a phase is attached to rays. The study is focused on the interaction process between structures and the surrounding acoustical medium. It is found that there exists six types of hybrid rays *i.e.* rays travelling in both structure and fluid.

The outline of the present paper is as follows. In Section 2, some general concepts such as ray field decomposition, the locality principle and canonical problems are introduced. These concepts are rather common in the literature in ray theories but here, they are described in the context of fluid–structure interaction. In Section 3, a review is done of all rays specific to radiation and absorption processes. This section is limited to these new rays and classical ones ever presented in the literature are not described. In Section 4, the relationships for fields attached to structural and acoustical rays are derived. Some relationships for the radii of curvature of wavefronts and the diffraction coefficients and are given in Sections 5 and 6. Finally, two applications are studied, radiation of sound from plates in Section 7 and transmission of sound through plates in Section 8.

2. General concepts

Rays are usually introduced as a first order development of the field in powers of $1/k$ where k is the wavenumber. The underlying assumption is that the field magnitude does not vary significantly over a wavelength. This condition usually applies at high frequencies that is when the wavelength is small compared with the typical length of system. In the case of vibrating plates immersed in a fluid, both wavelengths of structural and acoustical waves must be short.

The present study is limited to the interaction of vibration in plane plates with sound in air. In-plane motion in plates does not appear in the continuity equation at fluid–structure interface. The out-of-plane motion (flexural vibration) is therefore the only vibration directly responsible of interaction with fluid. However, in-plane motion may indirectly interact with fluid because of wave mode conversion during reflection at edges. But for the sake of simplicity, we shall not consider rays attached to in-plane waves. In the same spirit, creeping rays are not considered in what follows. Creeping rays are generated when an acoustical ray impinges on obstacle at grazing incidence. They are particularly important for curved structures but are of no importance for plane plates. Finally, the light fluid assumption will be systematically used after Section 6. The light fluid assumption allows the derivation of some simple closed-form relationships for diffraction coefficients avoiding the use of more general but more elaborated complex integrals.

A field is attached to each ray. And, at any point, the total field is simply obtained by summing all fields of individual rays passing through that point. Indeed, the nature of the field depends on the system. In fluid, the field is the acoustical pressure p whereas in structures, the field is the transverse displacement v. The choice of p and v for the field is not the only one possible. Other possibilities could be the acoustical potential, the transverse velocity of structure…Such another choice would not deeply modify the present analysis but only the expressions of diffraction coefficients.

An interesting consequence of the high frequency assumption is that all phenomena become local. Any interaction process involving several waves such as reflection, refraction, diffraction, only depends on the local geometry of the system and wavefronts. This is named the locality principle. The main interest of the locality principle is that the study of a complex problem involving several interaction processes may be split up into some simpler canonical problems. A canonical problem usually deals with a single difficulty. It has same local geometry as the complex problem, but extrapolated in such a manner that a closed-form solution is obtained. Many examples of canonical problems may be found in the related literature in optics or in acoustics. In Section 6, several references will be quoted for canonical problems related to vibroacoustics.

3. Review of rays in vibroacoustics

It is well-known that ray paths follow Fermat's principle. The law of reflection, equality of incidence and reflection angles, and Snell's law of refraction are all derived from this simple principle. But the most original contribution of the geometrical theory of diffraction is to extend this principle and to show the existence of many further kinds of rays such as diffracted rays, creeping rays and so some others.

Generalized Fermat's principle may be enunciated as follows. Consider a path between two points **a** and **b**. This path is assumed to be regular except at a point **p** where may occur reflection, refraction, or diffraction. This point **p** is constrained to be on a surface, edge, or vertex. We define the optical path L of the ray as the phase shift

$$L = \int k\mathbf{u}.\mathrm{d}\mathbf{s} \tag{1}$$

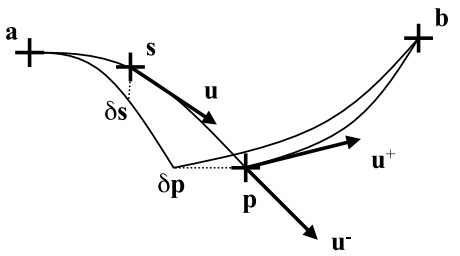

Fig. 1. Generalized Fermat's principle, the path **a**, **p**, **b** is stationary. The singular point **p** is constrained to lie on a surface, edge or vertex.

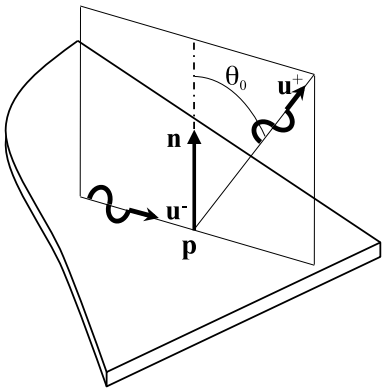

Fig. 2. Radiation of a supersonic structural ray, the acoustical ray starts with an emission angle θ_0 defined in Eq. (6).

where the integral is performed over the path $\mathbf{a}-\mathbf{p}-\mathbf{b}$, $\mathbf{u}$ is the unit vector tangent to the path, ω the circular frequency, c the phase speed, and $k=\omega/c$ the wavenumber which may vary along the path. Fermat's principle states that the actual optical path is stationary

$$\delta L = 0 \tag{2}$$

for infinitesimal variation $\delta\mathbf{s}$ of the path where **a** and **b** are fixed. By denoting $\mathbf{u}^-$, $\mathbf{u}^+$ the left and right unit vectors tangent to the singular point **p**, k^- (respectively k^+) the wavenumber on section $\mathbf{a}-\mathbf{p}$ (respectively $\mathbf{p}-\mathbf{b}$) (Fig. 1), integration by parts of Eq. (2) leads to

$$\int k\mathbf{u}.\mathrm{d}(\delta\mathbf{s}) = k^+\mathbf{u}.\delta\mathbf{b} - k^+\mathbf{u}^+.\delta\mathbf{p} + k^-\mathbf{u}^-.\delta\mathbf{p} - k^-\mathbf{u}.\delta\mathbf{a} - \int \delta\mathbf{s}.\mathrm{d}(k\mathbf{u}) = 0 \tag{3}$$

But $\delta\mathbf{a}=\delta\mathbf{b}=0$, it yields

$$\int \delta\mathbf{s}.\mathrm{d}(k\mathbf{u}) = 0 \quad \text{for all } \delta\mathbf{s} \tag{4}$$

$$(k^-\mathbf{u}^- - k^+\mathbf{u}^+).\delta\mathbf{p} = 0 \quad \text{for all } \delta\mathbf{p} \tag{5}$$

The first condition simplifies to $\mathrm{d}(k\mathbf{u}) = 0$. In homogeneous media ($k$ constant) $\mathbf{u}$ is constant and therefore the path is straight. The second relationship imposes a condition on position of point **p** that we shall investigate hereafter.

Let us now confine the discussion to vibroacoustics. A plane plate with normal $\mathbf{n}$ is immersed in a fluid. The subscript s refers to the structure (plate) and the subscript f to the fluid. We denote c_s the phase speed of structural rays and c_f that of sound rays.

Consider a structural ray travelling inside the plate in direction $\mathbf{u}^-$ as shown in Fig. 2. This ray may radiate a sound ray at point **p** in direction $\mathbf{u}^+$. When applying Eq. (5) to this situation, $\delta\mathbf{p}$ belongs to the plate plane. Since Eq. (5) applies for all $\delta\mathbf{p}$ verifying $\delta\mathbf{p}.\mathbf{n}=0$ then $\mathbf{u}^-/c_s - \mathbf{u}^+/c_f = \lambda\mathbf{n}$. In particular $\mathbf{u}^+$ belongs to the $\mathbf{u}^-$, $\mathbf{n}$-plane. Writing $\mathbf{u}^+ = \sin\theta_0\mathbf{u}^- + \cos\theta_0\mathbf{n}$, we get

$$\sin\theta_0 = \frac{c_f}{c_s} \tag{6}$$

It follows that a sound ray exists only if $c_s > c_f$, that is the structural ray is supersonic. The acoustical ray is then emitted in the plane $\mathbf{u}^-$, $\mathbf{n}$ with an emission angle θ_0.

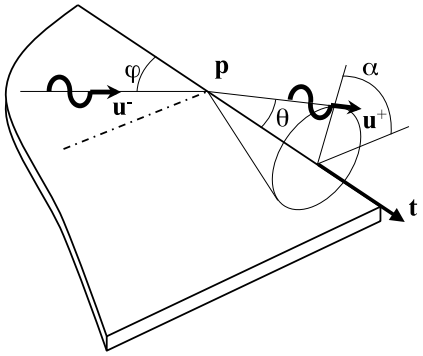

Fig. 3. Diffraction of a structural ray by edge, the acoustical ray lies in a Keller's cone which angle θ is given in Eq. (7).

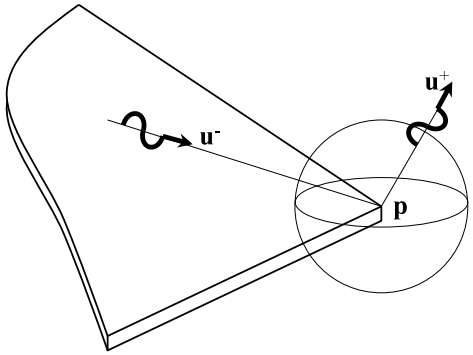

Fig. 4. Diffraction of a structural ray a corner, the acoustical ray may follow any direction.

Consider now a structural ray impinging on a plate edge with tangent vector $\mathbf{t}$ as shown in Fig. 3. The sound ray starts from the edge at a point $\mathbf{p}$. As $\delta\mathbf{p}$ is colinear to $\mathbf{t}$, $\delta\mathbf{p} = \lambda\mathbf{t}$ and Fermat's principle reads $(\mathbf{u}^-/c_s - \mathbf{u}^+/c_f).\mathbf{t} = 0$. By letting $\cos\varphi = \mathbf{u}^-.\mathbf{t}$ where φ is the incidence angle and $\cos\theta = \mathbf{u}^+.\mathbf{t}$ where θ is the elevation angle of emission, this reads

$$\cos\theta = \frac{c_f}{c_s}\cos\varphi \tag{7}$$

while the azimuthal angle of emission α can take any value. The diffracted ray belongs to Keller's cone of axis $\mathbf{t}$ and angle θ given by Eq. (7). Note that for supersonic structural ray ($c_s > c_f$), there is always a diffracted ray. But in the subsonic case, no diffraction occurs for incidence $\varphi < \arccos c_s/c_f$.

Finally, consider a structural ray impinging on a plate corner as shown in Fig. 4. The point $\mathbf{p}$ is fixed therefore $\delta\mathbf{p} = 0$. Eq. (5) is satisfied for any diffracted direction $\mathbf{u}^+$. A corner diffracts structural rays in all directions in the acoustical medium. More generally this is the case for any singular point such as force point, attachment point of additional mass or stiffness, or small hole.

By virtue of reciprocity, all previously determined paths can be inverted. It follows that acoustical rays hitting the plate with the particular incidence θ_0 are absorbed and transformed into structural rays. In a similar way, acoustical rays reaching a plate edge are also absorbed for any incidence in the subsonic case and incidence $\theta > \arccos c_f/c_s$ in the supersonic case. Finally, absorption by corner or any singular points occurs for any incidence.

Thus, there exists six types of hybrid rays *i.e.* rays travelling in both fluid and structure. They appear in vibroacoustics each time a structure radiates or absorbs acoustical energy. But all other classical rays may be required in practice.

4. Field of rays

In this section, fields attached to rays are derived. This calculation is performed in two separated steps, the field phase and its magnitude.

Along a ray, the phase shift $\Delta\varphi$ between two points separated by a distance r is simply the optical length

$$\Delta\varphi = k_\alpha r \tag{8}$$

where $k_\alpha = \omega/c_\alpha$ with $\alpha = s,\ f$.

The magnitude of the field is determined by applying the principle of conservation of energy in a ray beam.

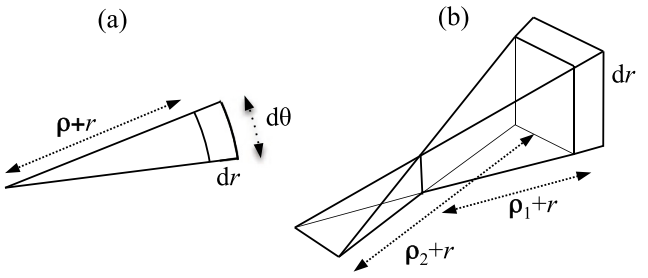

Fig. 5. Energy balance in a beam of rays, (a) in plate, (b) in fluid.

Consider first the case of a plate and a ray beam of angle $\mathrm{d}\theta$ as shown in Fig. 5a. The structural intensity is denoted by I. If the wavefront has radius of curvature ρ, all rays passing through that wavefront stem from a same point located at distance ρ in normal direction behind the wavefront. At a distance r (resp. $r+\mathrm{d}r$) ahead of the wavefront, the radius of curvature is $\rho+r$ (resp. $\rho+r+\mathrm{d}r$). In the infinitesimal element $(\rho+r)\mathrm{d}r\mathrm{d}\theta$, the ingoing power is $(\rho+r)I\mathrm{d}\theta$ whereas the outgoing power is $(\rho+r+\mathrm{d}r)(I+\mathrm{d}I)d\theta$. Dissipation by structural damping induces a dissipated power proportional to $(\rho+r)Id\theta\mathrm{d}r$. Similarly, sound radiation imposes an additional loss. Let $2m_s$ be the total attenuation factor. Neglecting second order terms, the energy balance reads

$$\frac{\mathrm{d}I}{\mathrm{d}r}+\frac{1}{\rho+r}I(r)+2m_sI(r)=0 \tag{9}$$

with the solution

$$I(r)=I(0)\frac{\rho}{\rho+r}\exp(-2m_sr) \tag{10}$$

A ray is a travelling wave. In particular the proportionality $I\propto|v|^2$ holds where v is the plate deflection. Since, $|v|\propto\sqrt{I}$ and the phase of v is given in Eq. (8), we finally obtain the deflection field as

$$v(r)=v(0)\sqrt{\frac{\rho}{\rho+r}}\exp(\mathrm{i}\bar{k}_sr) \tag{11}$$

where $\mathrm{i}=\sqrt{-1}$ and $\bar{k}_s=k_s+\mathrm{i}m_s$ is the complex structural wavenumber. In Appendix A, some explicit relationships for k_s and m_s are given in both cases of subsonic and supersonic waves.

In the case of acoustical rays, an additional difficulty arises from the presence of two principal radii of curvature for wavefronts. Let denote by ρ_1 and ρ_2 these radii. At a distance r (resp. $r+\mathrm{d}r$) ahead of the wavefront the radii becomes ρ_1+r and ρ_2+r (resp. $\rho_1+r+\mathrm{d}r$ and $\rho_2+r+\mathrm{d}r$) as shown in Fig. 5b. Considering that acoustical rays loss some energy due to the atmospheric absorption with an attenuation factor m_f, the energy balance is

$$\frac{\mathrm{d}I}{\mathrm{d}r}+\frac{1}{\rho_1+r}I(r)+\frac{1}{\rho_2+r}I(r)+2m_fI(r)=0 \tag{12}$$

with the solution

$$I(r)=I(0)\frac{\rho_1\rho_2}{(\rho_1+r)(\rho_2+r)}\exp(-2m_fr) \tag{13}$$

Finally, the pressure field p is obtained by

$$p(r)=p(0)\sqrt{\frac{\rho_1\rho_2}{(\rho_1+r)(\rho_2+r)}}\exp(\mathrm{i}\bar{k}_fr) \tag{14}$$

where $\bar{k}_f=k_f+\mathrm{i}m_f$ is the complex acoustical wavenumber. This field is a spherical wave when $\rho_1=\rho_2$, a cylindrical wave when $\rho_2\to\infty$ and a plane wave when $\rho_1\to\infty,\ \rho_2\to\infty$.

5. Radius of curvature

Let us examine how the wavefronts are transformed during a fluid–structure interaction. A wavefront is determined by the principal radii of curvature but also the orientation of the principal directions in the plane normal to the ray. In general, fluid–structure interaction modifies the ray direction, the principal directions of wavefront, and the principal radii of curvature. Since the modification of ray direction has been outlined in Section 3, the remaining question is therefore to determine the principal directions and the curvatures of wavefronts after transformation.

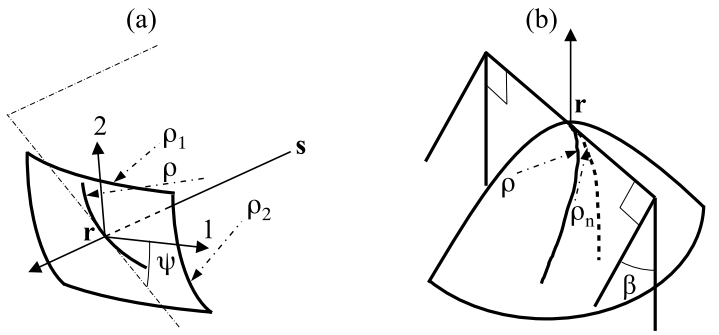

Fig. 6. Geometry of wavefront. (a) Euler's formula: 1 and 2 principal directions; ρ_1, ρ_2 principal radii of curvature; ρ radius of curvature in a normal plane inclined by ψ to direction 1. (b): Meusnier's theorem: ρ_n radius of curvature in normal plane; ρ radius of curvature in a plane inclined by β to the normal plane.

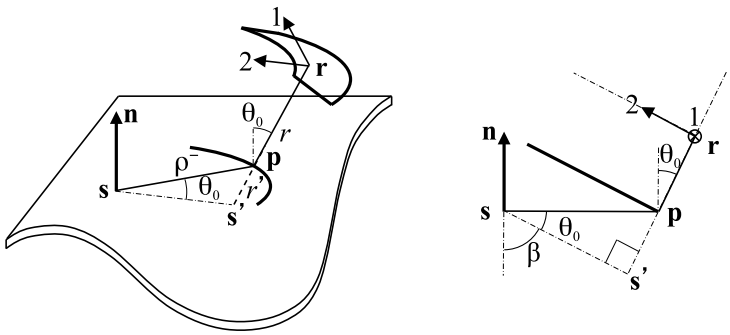

Fig. 7. Wavefronts for supersonic structural ray radiating acoustical rays. The acoustical wavefront at **r** is a cone of axis **n** with a straight generating line normal to the ray.

Wavefronts are defined as surfaces of all points of the bundle rays having same phase (Fig. 6a). A wavefront is normal to the ray direction. For each normal plane defined by the ray direction and any transverse direction, the intersection with the wavefront forms a curve whose radius of curvature is noted ρ. The principal directions 1 and 2 are the two transverse directions for which the radii of curvatures ρ_1 and ρ_2 reach their maximum and minimum values. The principal directions are orthogonal. If a normal plane is inclined by ψ relative to direction 1, the radius of curvature ρ verifies Euler's formula $1/\rho = \cos^2\psi/\rho_1 + \sin^2\psi/\rho_2$. Another important result is the so-called Meusnier's theorem (Fig. 6b). Let ρ_n be the radius of curvature at **r** in a normal plane and ρ the radius of curvature of the curve intersection with a plane that makes angle α with the normal and has the same tangent at **r**. Then Meusnier's theorem states that $\rho = \rho_n \cos\beta$.

Let us consider the case of an acoustical ray radiated by a supersonic structural ray. Assuming that the radius of curvature of the structural wavefront at point **p** is ρ^- (Fig. 7), the optical path from the source **s** to **p** is $k_s\rho^-$. In the fluid, the ray seems to stem from a point **s**′ located below the plate at a distance $r' = \rho^- k_s/k_f = \rho^- \sin\theta_0$ (after Eq. (7)) in the radiated direction. The set of all points **s**′ for various points **p** forms a cone of vertex **s**, axis **n** and half-angle $\beta = \pi/2 - \theta_0$. Since the acoustical path from **s**′ to **p** equals the structural path from **s** to **p**, **s**′ has same phase as **s**. This cone is therefore an equiphase surface. The acoustical wavefront at **p** being an equiphase surface is also a cone of same axe and half-angle. The principal directions of this cone are firstly, the tangent in the plate plane (this is also the tangent to the structural wavefront at **p**) and secondly the generating line passing through **p**. The calculation of the curvatures of a cone is classical. Meusnier's theorem states that the radius of curvature in the section normal to the generating line at **p** is $\rho_1^+ = \rho^-/\cos\beta$ since ρ^- is the radius of the circle normal to **n** of centre **s**. This gives the first principal curvature. The second principal curvature is zero since the generating line of a cone is straight. The radii of curvature in the principal directions are therefore

$$\rho_1^+ = \rho^-/\sin\theta_0 \tag{15}$$

$$\rho_2^+ = \infty \tag{16}$$

Setting $\rho_2^+ \to \infty$ in Eq. (14), the pressure field at a point **r** located at distance r from **p** in direction θ_0 (Fig. 7) is

$$p(\mathbf{r}) = p(\mathbf{p})\sqrt{\frac{\rho_1^+}{\rho_1^+ + r}}\exp(\mathrm{i}\bar{k}_f r) \tag{17}$$

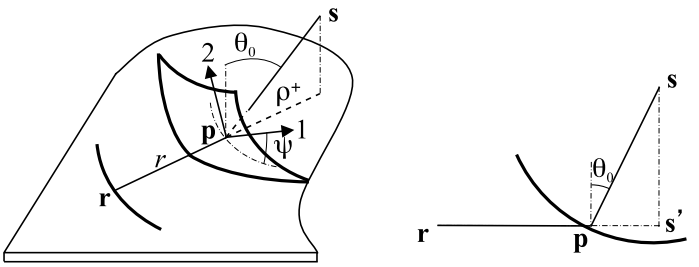

Fig. 8. Wavefronts for acoustical rays under incidence θ_0 converted into structural rays. The structural wavefront at **p** is the curve intersection of the incident acoustical wavefront and the plate.

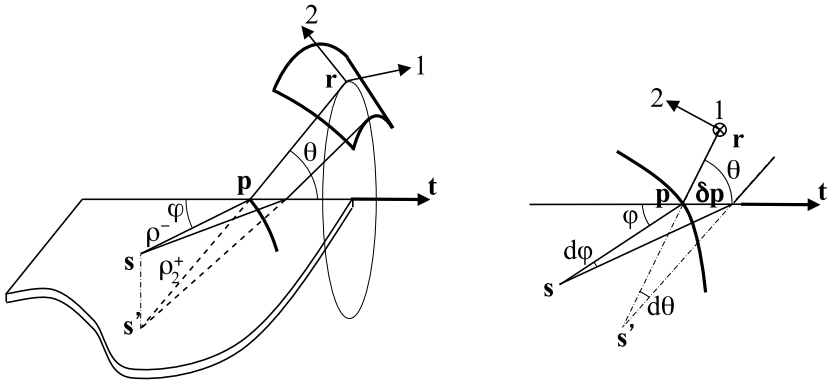

Fig. 9. Wavefronts for structural rays diffracted by edges. The acoustical wavefront at **r** is a cone of axis **t** with a curved generating line.

Now substituting the above value of ρ_1^+ and defining the detachment coefficient L_f such that $p(\mathbf{p}) = L_f v(\mathbf{p})$ where $v(\mathbf{p})$ is the transverse deflection at **p**, it yields

$$p(\mathbf{r}) = v(\mathbf{p}) L_f \sqrt{\frac{\rho^-}{\rho^- + r\sin\theta_0}}\exp(\mathrm{i}\bar{k}_f r) \tag{18}$$

The detachment coefficient L_f will be determined in Section 6.

The reciprocal problem is easier (Fig. 8). When an acoustical ray impinges on the plate at incidence θ_0, all points located on the intersection of the incident acoustical wavefront and the plate plane have same phase. This curve is therefore the wavefront of the structural ray. Consider the normal plane defined by the ray direction and the tangent to wavefront at **p** in the plate plane. Let us denote ρ^- the radius of curvature of the acoustical wavefront in this normal plane. If this normal plane makes angle ψ with the principal direction 1 of the incident wavefront, then by Euler's formula $1/\rho^- = \cos^2\psi/\rho_1^- + \sin^2\psi/\rho_2^-$ with ρ_1^-, ρ_2^- being the radii of curvature in principal directions. Now, let ρ^+ be the radius of curvature at **p** of the curve intersection of wavefront and plate plane. By Meusnier's theorem

$$\rho^+ = \rho^- \sin\theta_0 \tag{19}$$

After Eq. (11), the structural field at a point **r** at distance r from **p** (Fig. 8), is then

$$v(\mathbf{r}) = p(\mathbf{p}) L_s \sqrt{\frac{\rho^- \sin\theta_0}{\rho^- \sin\theta_0 + r}}\exp(\mathrm{i}\bar{k}_s r) \tag{20}$$

where L_s is the attachment coefficient defined by $v(\mathbf{p}) = L_s p(\mathbf{p})$ (see Section 6).

When a structural ray is diffracted into the fluid by an edge, we denote by ρ^- the radius of curvature of the structural wavefront in the plate plane at point **p** on the edge (Fig. 9). We must determine the principal directions of the acoustical wavefront and their normal radius of curvatures noted ρ_1^+ and ρ_2^+. All acoustical rays in the Keller's cone start with same initial phase. The circles normal to the edge (axis of the cone) are thus equiphased. The radius of curvature equals the circle radius, and since **p** is the vertex of Keller's cone, we get $\rho_1^+ = 0$. In addition, in the fluid, the ray seems to start from a fictitious source $\mathbf{s}'$ located below **p** in the diffracted direction. The distance $\rho_2^+ = |\mathbf{p} - \mathbf{s}'|$ is given by the following argument. Consider an infinitesimal variation $\delta\mathbf{p}$ of the diffracting point on the edge. The variation $\mathrm{d}\varphi$ of incidence is given by $|\delta\mathbf{p}| = \rho^- \mathrm{d}\varphi/\sin\varphi$ where φ is the incidence angle. In the same way, this must equal the variation for the corresponding infinitesimal angle $\mathrm{d}\theta$

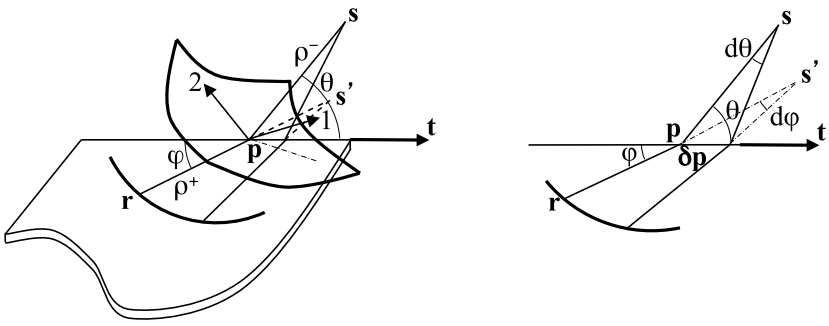

Fig. 10. Wavefronts for acoustical rays diffracted into structural rays by plate edges.

where θ is the emission angle. So, $\rho^- \mathrm{d}\varphi/\sin\varphi = \rho_2^+ \mathrm{d}\theta/\sin\theta$ and finally, differentiating Eq. (7), it yields

$$\rho_1^+ = 0 \tag{21}$$

$$\rho_2^+ = \rho^- \frac{k_f}{k_s} \frac{\sin^2\theta}{\sin^2\varphi} \tag{22}$$

The wavefront is therefore a cone about the edge with a curved generating line. The principal directions are drawn in Fig. 9. Following Eq. (14), the pressure field in the fluid at a point $\mathbf{r}$ distant from $\mathbf{p}$ by r in direction θ is

$$p(\mathbf{r}) = v(\mathbf{p}) D_f^{\text{edge}} \sqrt{\frac{\rho^- k_f \sin^2\theta}{(\rho^- k_f \sin^2\theta + r k_s \sin^2\varphi) r}} \exp(\mathrm{i}\bar{k}_f r) \tag{23}$$

where D_f^{edge} is a diffraction coefficient defined by $p(\mathbf{p}) = D_f^{\text{edge}} v(\mathbf{p})$.

Consider now the case of an acoustical ray hitting a plate edge and diffracted into a structural ray (Fig. 10). Let ρ^- be the radius of curvature of incident wavefront in the normal plane containing the edge and the incident ray. If this plate makes angle ψ with the principal direction 1 then by Euler's formula $1/\rho^- = \cos^2\psi/\rho_1^- + \sin^2\psi/\rho_2^-$. ρ^+ denotes the radius of curvature of the structural wavefront at $\mathbf{p}$. Following the same reasoning as in the previous case, an infinitesimal variation of $\mathbf{p}$ is $|\delta\mathbf{p}| = \rho^- \mathrm{d}\theta/\sin\theta = \rho^+ \mathrm{d}\varphi/\sin\varphi$. Finally,

$$\rho^+ = \rho^- \frac{k_s}{k_f} \frac{\sin^2\varphi}{\sin^2\theta} \tag{24}$$

And the field for the structural ray is by Eq. (11)

$$v(\mathbf{r}) = p(\mathbf{p}) D_s^{\text{edge}} \sqrt{\frac{\rho^- k_s \sin^2\varphi}{\rho^- k_s \sin^2\varphi + r k_f \sin^2\theta}} \exp(\mathrm{i}\bar{k}_s r) \tag{25}$$

where D_s^{edge} is a diffraction coefficient defined by $v(\mathbf{p}) = D_s^{\text{edge}} p(\mathbf{p})$.

When a structural ray is diffracted into fluid by a corner or a singularity, the diffracted wavefront is spherical and so, both radii of curvature are zero at the diffraction point

$$\rho_1^+ = 0 \tag{26}$$

$$\rho_2^+ = 0 \tag{27}$$

The diffracted field is thus by Eq. (14)

$$p(\mathbf{r}) = v(\mathbf{p}) D_f^{\text{corner}} \frac{1}{r} \exp(\mathrm{i}\bar{k}_f r) \tag{28}$$

which does not depend on the radius of curvature of incident wavefront. D_f^{corner} is a diffraction coefficient defined by $p(\mathbf{p}) = D_f^{\text{corner}} v(\mathbf{p})$.

Conversely, when an acoustical ray is diffracted into the structure by a corner, the structural diffracted ray is cylindrical and thus

$$\rho^+ = 0 \tag{29}$$

By Eq. (11), the field at a point $\mathbf{r}$ distant by r from the corner, is

$$v(\mathbf{r}) = p(\mathbf{p}) D_s^{\text{corner}} \frac{1}{\sqrt{r}} \exp(\mathrm{i}\bar{k}_s r) \tag{30}$$

where D_s^{corner} is a diffraction coefficient defined by $v(\mathbf{p}) = D_s^{\text{corner}} p(\mathbf{p})$.

6. Diffraction coefficients

This section gives explicit relationship for the detachment coefficient L_f, the attachment coefficient L_s, and the diffraction coefficients D_f^{edge} and D_s^{edge}. Other coefficients useful in practice are also provided. For each coefficient, we specify a reference or give the complete calculation in appendices. From now, the light fluid assumption will always be admitted. The time convention is $\exp(-\mathrm{i}\omega t)$.

In this section, we shall denote by ρ_0 the density of the light fluid (air) and $k_f = \omega/c_f$ the acoustical wavenumber where c_f is the sound speed. The plate is thin and has bending stiffness $B = Eh^3/12(1-\nu^2)$ where E is Young's modulus, h the plate thickness and ν the Poisson coefficient. The plate has mass per unit area m. At frequency ω, the structural wavenumber is $k_s = (m\omega^2/B)^{1/4}$ and the phase speed in plate is $c_s = (B\omega^2/m)^{1/4}$.

The problem of a supersonic structural ray radiating sound rays during its travel, shown in Fig. 2, exhibits a detachment coefficient L_f in Eq. (18). This coefficient is calculated by considering the canonical problem of a structural plane travelling in an infinite plate and radiating a sound plane wave. This canonical problem is classical in the literature (see for instance [18], page 502). The sound plane wave is emitted at angle θ_0 and its magnitude may be calculated by applying the continuity condition at the fluid–plate interface. L_f is determined by $p = L_f v$ where p and v are respectively the pressure and plate deflection waves. With the above notations, this gives the following detachment coefficient for sound radiation

$$L_f = \frac{-\mathrm{i}\rho_0\omega^2}{\sqrt{k_f^2 - k_s^2}} \tag{31}$$

when $c_s > c_f$ and zero otherwise. Note that L_f is a complex number. This value of L_f must be substituted in Eq. (18).

In the reciprocal problem, a sound ray hits the plate at incidence θ_0 and transformed into a structural ray. The canonical problem, a sound plane wave impinging on an infinite plate at incidence θ_0 and giving rise to a structural plane wave, is strictly equivalent to the previous canonical problem of sound radiation, excepted that the time must be reversed. The attachment coefficient L_s which appears in Eq. (20) is then obtained by applying $v = L_s p$ where v is the plate deflection and p the acoustical pressure on the plate surface. It yields

$$L_s = -\frac{1}{L_f} \tag{32}$$

Note that the minus sign comes from the time inversion (formally equivalent to the substitution $\mathrm{i} \to -\mathrm{i}$). This value of L_s must be substituted in Eq. (20).

In the third problem, a structural ray impinging on a plate edge at incidence φ is diffracted into the fluid as shown in Fig. 3. The associated canonical problem considers a structural plane wave impinging on the straight edge of a semi-infinite plate. The structural wave is both reflected into the plate and diffracted into the fluid. The following values of the reflection coefficient defined as the ratio of reflected to incident plane wave magnitudes, are calculated by assuming that the plate is *in vacuo* (see Appendix B for details).

$$R_s = -1 \qquad \text{for simply supported edge} \tag{33}$$

$$R_s = \frac{\sin\varphi + \mathrm{i}\sqrt{1+\cos^2\varphi}}{\sin\varphi - \mathrm{i}\sqrt{1+\cos^2\varphi}} \qquad \text{for clamped edge} \tag{34}$$

$$R_s = \frac{-\mathrm{i}\frac{\sqrt{1+\cos^2\varphi}}{\sin\varphi}\left[1-(1-\nu)\cos^2\varphi\right]^2 - \left[1+(1-\nu)\cos^2\varphi\right]^2}{\mathrm{i}\frac{\sqrt{1+\cos^2\varphi}}{\sin\varphi}\left[1-(1-\nu)\cos^2\varphi\right]^2 - \left[1+(1-\nu)\cos^2\varphi\right]^2} \qquad \text{for free edge} \tag{35}$$

An evanescent wave is also reflected in the plate by the edge. In the same condition, the reflection coefficients for this evanescent wave are

$$R_e = 0 \qquad \text{for simply supported edge} \tag{36}$$

$$R_e = \frac{-2\sin\varphi}{\sin\varphi - \mathrm{i}\sqrt{1+\cos^2\varphi}} \qquad \text{for clamped edge} \tag{37}$$

$$R_e = \frac{2\left[1-(1-\nu)^2\cos^4\varphi\right]}{-\mathrm{i}\frac{\sqrt{1+\cos^2\varphi}}{\sin\varphi}\left[1-(1-\nu)\cos^2\varphi\right]^2 + \left[1+(1-\nu)\cos^2\varphi\right]^2} \qquad \text{for free edge} \tag{38}$$

Note that the *in vacuo* assumption only gives a zero-order approximation of the actual reflection coefficients in the presence of a fluid loading. In particular from Eqs. (33), (34), (35), we get $|R_s|^2 = 1$ which shows that all energy is reflected into the plate. These reflection coefficient will turn out to be useful when we will consider the radiation problem in Section 7 and the transmission problem in Section 8.

The diffraction coefficient D_f^{edge} in Eq. (23) is obtained by solving the same canonical problem of a structural plane wave impinging on the edge of a plate at incidence φ (see Fig. 3). The rigorous solution to this canonical problem requires the application of the Wiener–Hopf technique (see [19–21] for a complete solution with various boundary conditions). We

give below a version of D_f^{edge} which follows the simplified method described in [22,23]. It is obtained under the light fluid assumption by solving the Helmholtz equation with *in vacuo* deflection field as boundary conditions. The plate is assumed to be baffled. The polar angle about the edge is noted α (Fig. 3) and the incidence angle φ. We have seen in Section 3 that no ray is diffracted when $\varphi < \arccos c_s/c_f$, we can therefore assume that $k_f > k_s \cos\varphi$. The diffraction coefficient is then

$$D_f^{\text{edge}}(\varphi,\alpha) = -\rho_0\omega^2 \frac{\hat{u}(k_f \sin\theta\cos\alpha)}{\sin\theta\sqrt{2\pi k_f}} \exp\left(\mathrm{i}\frac{\pi}{4}\right) \tag{39}$$

where the function $\hat{u}$ is

$$\hat{u}(s) = \frac{-\mathrm{i}}{k_s\sin\varphi - s} + \frac{\mathrm{i}R_s}{k_s\sin\varphi + s} + \frac{R_e}{k_s(1+\cos^2\varphi)^{1/2} - \mathrm{i}s} \tag{40}$$

In these relationships, the emission angle θ is related to incidence angle φ by Eq. (7). This value of D_f^{edge} may be substituted in Eq. (23).

In the fourth problem, the reciprocal of the third one, an acoustical ray hits the plate edge and is diffracted in both structural ray and acoustical rays. The corresponding canonical problem is an acoustical plane wave hitting an edge of a semi-infinite plate with incidence θ tangent to the edge and polar angle α (Fig. 3). Again, a rigorous solution is a problem of complex analysis. In [22], it is proposed to estimate the diffracted field under the light fluid assumption by remarking that the incident sound wave imposes a forced field in the plate which does not satisfy the plate boundary conditions. The method consists in enforcing the boundary conditions of the plate by adding a structural plane wave of wavenumber k_f and an evanescent wave, both in direction φ. The diffraction coefficient D_s^{edge} is the magnitude of this structural plane wave

$$D_s^{\text{edge}}(\theta,\alpha) = \frac{\mathrm{i}[1+\cos^2\varphi + (\frac{k_f}{k_s}\sin\theta\cos\alpha)^2]k_f\sin\theta\sin\alpha}{2\rho_0\omega^2 + \mathrm{i}B[k_f^4(1-\sin^2\theta\sin^2\alpha)^2 - k_s^4]k_f\sin\theta\sin\alpha} \tag{41}$$

for simply supported edge. The emission angle φ is related to incidence angle θ by Eq. (7). This diffraction coefficient appears in Eq. (25).

Unfortunately, the canonical problem of a structural plane wave hitting a corner or any other singularity of a plate has not been solved analytically. No simple expression for the corresponding acoustical diffraction coefficient are available in the literature. Similarly, the reciprocal canonical problem of an acoustical plane wave hitting a corner has not been solved. Especially, the diffraction coefficient attached to structural waves emanating from the edge is unknown.

Other diffraction or reflection coefficients are useful in practice. For instance, in the example of sound transmission that will be discussed in Section 8, we shall need to consider the problem of a sound ray hitting a plate and split into reflected and transmitted rays. The associated canonical problem is a sound plane wave impinging on a thin infinite plate with incidence θ normal to the plate. This is a standard problem in the literature. The reflection and transmission coefficients are (see for instance [13], page 232)

$$R_f(\theta) = \frac{\mathrm{i}[B(k_f\sin\theta)^4 - m\omega^2]k_f\cos\theta}{2\rho_0\omega^2 + \mathrm{i}[B(k_f\sin\theta)^4 - m\omega^2]k_f\cos\theta} \tag{42}$$

$$T_f(\theta) = \frac{2\rho_0\omega^2}{2\rho_0\omega^2 + \mathrm{i}[B(k_f\sin\theta)^4 - m\omega^2]k_f\cos\theta} \tag{43}$$

A final problem that may be of practical interest is a fluid loaded plate excited by a transverse point force. Under such a concentrated excitation, two waves emanate from the driven point. The structural wave is cylindrical $v(r) = A_s\exp(\mathrm{i}k_s r)/\sqrt{r}$ where r is the source-receiver distance. The acoustical wave is spherical of the form $p(r) = A_f\exp(\mathrm{i}k_f r)/r$. The amplitudes $A_\alpha, \alpha = s, f$ have been calculated under the light fluid assumption in [18,24]. They will not be used in the rest of this paper.

7. Radiation of sound

In this section, we detail a simple application of GTD to a sound radiation problem.

We consider a structural plane wave incident on the edge of a semi infinite baffled plate as shown in Fig. 11. Let $\mathbf{r}$ denote a point above the plate. To determine the acoustical pressure at this point, we need to make an inventory of all rays passing through that point. First, the incident ray is diffracted by the edge leading to the field p_1. Since any point in the fluid is located on a unique Keller's cone, the point $\mathbf{r}$ is always reached by such a diffracted ray. Secondly, in the supersonic frequency range, the incident structural ray radiates continuously acoustical rays at angle θ_0 which may reach the reception point $\mathbf{r}$. The attached field is noted p_2. Finally, the incident ray is reflected by the edge and the resulting reflected plane wave also radiates acoustical rays at angle $-\theta_0$ whose field is noted p_3. Three zones are thus clearly defined depending on the number of rays reaching $\mathbf{r}$. They are summarized as follows.

- zone I: $p(\mathbf{r}) = p_1(\mathbf{r})$
- zone II: $p(\mathbf{r}) = p_1(\mathbf{r}) + p_2(\mathbf{r})$
- zone III: $p(\mathbf{r}) = p_1(\mathbf{r}) + p_2(\mathbf{r}) + p_3(\mathbf{r})$

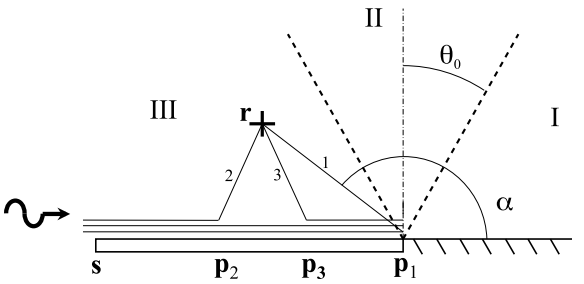

Fig. 11. Plane wave hitting the edge of a plate. Three rays are radiated towards the fluid and three zones numbered in Roman characters are defined depending on the number of rays reaching the zone.

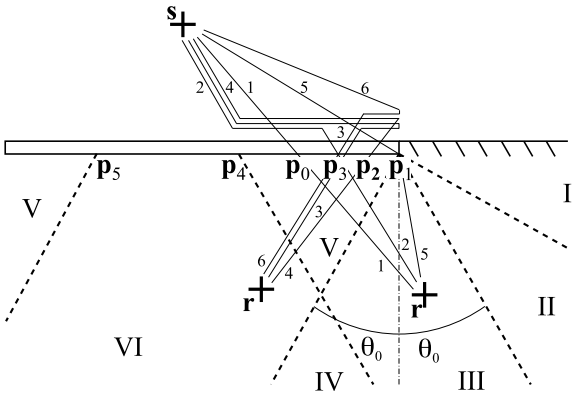

Fig. 12. Cylindrical wave hitting the plate. Six rays are transmitted through the plate and six zones numbered in Roman characters are defined depending on the number of rays reaching the zone.

These zones and the three types of acoustical rays are shown in Fig. 11.

Now, let us calculate the field attached to each ray. The incident structural ray is assumed to be a plane wave with a unit magnitude ($\rho^- = \infty$). Firstly, the diffracted field is by Eq. (23)

$$p_1(\mathbf{r}) = \exp(\mathrm{i}\bar{k}_s d_1) D_f^{\text{edge}}(\alpha) \frac{\exp(\mathrm{i}\bar{k}_f r_1)}{\sqrt{r_1}} \tag{44}$$

where $d_1 = |\mathbf{p}_1 - \mathbf{s}|$ and $r_1 = |\mathbf{p}_1 - \mathbf{r}|$. The term $\exp(\mathrm{i}\bar{k}_s d_1)$ is attached to the structural part of the ray while $D_f^{\text{edge}} \exp(\mathrm{i}\bar{k}_f r_1)/\sqrt{r_1}$ is the cylindrical acoustical wave from the edge to the receiver point. Secondly, the field radiated by the incident ray is by Eq. (18)

$$p_2(\mathbf{r}) = \exp(\mathrm{i}\bar{k}_s d_2) L_f \exp(\mathrm{i}\bar{k}_f r_2) \tag{45}$$

where $d_2 = |\mathbf{p}_2 - \mathbf{s}|$ and $r_2 = |\mathbf{p}_2 - \mathbf{r}|$. L_f is the factor for radiation and $\exp(\mathrm{i}\bar{k}_f r_2)$ the field attached to the acoustical plane wave. Thirdly, the field radiated by the reflected ray is

$$p_3(\mathbf{r}) = \exp(\mathrm{i}\bar{k}_s d_1) R_s \exp(\mathrm{i}\bar{k}_s d_3) L_f \exp(\mathrm{i}\bar{k}_f r_3) \tag{46}$$

where $d_3 = |\mathbf{p}_3 - \mathbf{p}_1|$ and $r_3 = |\mathbf{p}_3 - \mathbf{r}|$. The term $R_s \exp(\mathrm{i}\bar{k}_s d_3)$ is due to the reflected field.

This simple example illustrates the ease with which a ray-tracing approach applies to sound radiation problems. Of course, the semi-infinite nature of the plate leads a small number of rays. In the case of a finite plate, successive reflections occur on plates edges and the fields are series of structural rays radiating sound rays. An energetic approach to this problem is presented in [25,26].

8. Transmission of sound

The second application is concerned with a transmission problem. Consider a cylindrical acoustical wave emanating from the source point **s** and impinging on a semi-infinite baffled plate as shown in Fig. 12. One searches the acoustical field in the lower half-plane. From the source **s** to the receiver point **r**, six rays can propagate. The first one is the acoustical ray that

reaches the receiver point in straight line directly through the plate. The field is noted p_1 with

$$p_1(\mathbf{r}) = \frac{\exp(\mathrm{i}\bar{k}_f s_0)}{\sqrt{s_0}} T_f \frac{\sqrt{s_0}}{\sqrt{s_0 + r_0}} \exp(\mathrm{i}\bar{k}_f r_0) \tag{47}$$

where $s_0 = |\mathbf{p}_0 - \mathbf{s}|$ and $r_0 = |\mathbf{p}_0 - \mathbf{r}|$. The second ray is absorbed by the structure at incidence θ_0, travels in the plate, and is radiated into the lower fluid with emission angle θ_0. The corresponding field is

$$p_2(\mathbf{r}) = \frac{\exp(\mathrm{i}\bar{k}_f s_4)}{\sqrt{s_4}} L_s \exp(\mathrm{i}\bar{k}_s d_1) L_f \exp(\mathrm{i}\bar{k}_f r_3) \tag{48}$$

where $s_4 = |\mathbf{p}_4 - \mathbf{s}|$, $r_3 = |\mathbf{p}_3 - \mathbf{r}|$ and $d_1 = |\mathbf{p}_4 - \mathbf{p}_3|$. The third one is similar to the second one, although it is reflected by the edge before to be radiated.

$$p_3(\mathbf{r}) = \frac{\exp(\mathrm{i}\bar{k}_f s_4)}{\sqrt{s_4}} L_s \exp(\mathrm{i}\bar{k}_s d_2) R_s \exp(\mathrm{i}\bar{k}_s d_3) L_f \exp(\mathrm{i}\bar{k}_f r_2) \tag{49}$$

where $r_2 = |\mathbf{p}_2 - \mathbf{r}|$, $d_2 = |\mathbf{p}_1 - \mathbf{p}_4|$ and $d_3 = |\mathbf{p}_1 - \mathbf{p}_2|$. The fourth ray is successively absorbed at incidence θ_0 and diffracted by the edge.

$$p_4(\mathbf{r}) = \frac{\exp(\mathrm{i}\bar{k}_f s_4)}{\sqrt{s_4}} L_s \exp(\mathrm{i}\bar{k}_s d_2) D_f^{\mathrm{edge}} \frac{\exp(\mathrm{i}\bar{k}_f r_1)}{\sqrt{r_1}} \tag{50}$$

where $r_1 = |\mathbf{p}_1 - \mathbf{r}|$. The fifth one is the acoustical ray impinging on the edge and directly diffracted towards the receiver point.

$$p_5(\mathbf{r}) = \frac{\exp(\mathrm{i}\bar{k}_f s_1)}{\sqrt{s_1}} D_f^{\mathrm{edge}} \frac{\exp(\mathrm{i}\bar{k}_f r_1)}{\sqrt{r_1}} \tag{51}$$

with $s_1 = |\mathbf{p}_1 - \mathbf{s}|$. Finally, the sixth ray is diffracted into the structure by the edge, travels into the structure and is radiated with emission angle θ_0 towards the receiver point. Its field is

$$p_6(\mathbf{r}) = \frac{\exp(\mathrm{i}\bar{k}_f s_1)}{\sqrt{s_1}} D_s^{\mathrm{edge}} \exp(\mathrm{i}\bar{k}_s d_3) L_f \exp(\mathrm{i}\bar{k}_f r_2) \tag{52}$$

These rays do not reach every point of the lower half-plane and the pattern. They are summarized as follows.

- zone I: $p(\mathbf{r}) = p_4 + p_5$
- zone II: $p(\mathbf{r}) = p_1 + p_4 + p_5$
- zone III: $p(\mathbf{r}) = p_1 + p_2 + p_4 + p_5$
- zone IV: $p(\mathbf{r}) = p_1 + p_4 + p_5$
- zone V: $p(\mathbf{r}) = p_1 + p_2 + p_3 + p_4 + p_5 + p_6$
- zone VI: $p(\mathbf{r}) = p_1 + p_3 + p_4 + p_5 + p_6$

These zones and the three types of acoustical rays are shown in Fig. 12.

9. Conclusion

In this paper, the geometrical theory of diffraction has been applied to sound radiation and structural response of plane structures. It has been shown that fluid–structure interaction gives rise to six structural–acoustical rays. These are radiation of supersonic structural rays, diffraction by edges of structural rays, diffraction by corners of structural rays, absorption of acoustical rays at incidence θ_0, absorption of acoustical rays by edges, absorption of acoustical rays by corners. Some of these rays may not exist in particular situations. Their existence are specified by Snell's laws derived from Fermat's principle. In practice, a complete description of a problem requires all other classical rays such as structural–structural rays reflected by edges, diffracted by corners and acoustical–acoustical rays reflected by plates, transmitted through plates, diffracted by edges, corners, creeping rays and so on.

Acknowledgements

The author would like to thank V. Cotoni for the fruitful debates on ray theories, energetic approaches and the solving of canonical problems. This work was supported by the CNRS and Labex CeLyA of Université de Lyon, France, operated by the French National Research Agency (ANR-10-LABX-0060/ANR-11-IDEX-0007). This support is greatly appreciated.

Appendix A

In this Appendix some basic relationships related to the fluid–structure interaction are derived. The plate has mass per unit area m and bending stiffness $B = Eh^3/12(1-\nu^2)$ where E is Young's modulus, h the plate thickness and ν Poisson's coefficient. The circular frequency is noted ω and the time convention is $\exp(-\mathrm{i}\omega t)$. The *in vacuo* the plate wavenumber is $k_v = (m\omega^2/B)^{1/4}$. The fluid has volumic mass ρ_0 and speed of sound c_f. The wavenumber of acoustical waves is $k_f = \omega/c_f$. In the presence of material damping, a complex wavenumber is introduced. For the plate, $\bar{k}_v = k_v(1+\mathrm{i}\eta/4)$ where η is the damping loss factor of the material. In the fluid, $\bar{k}_f = k_f + \mathrm{i}m_f$ where m_f is the sound absorption coefficient. When the coupling between plate and fluid is taken into account, the structural wavenumber is no longer $\bar{k}_v$ but $\bar{k}_s$. The continuity of velocity on the plate gives the dispersion equation

$$B(\bar{k}_s^4 - \bar{k}_v^4) = \frac{-2\mathrm{i}\rho_0\omega^2}{(\bar{k}_f^2 - \bar{k}_s^2)^{1/2}} \tag{A.1}$$

This equation has five solutions for $\bar{k}_s$ but only one is physical corresponding to a decreasing travelling wave. The real wavenumber k_s and the absorption coefficient m_s are simply obtained by separating the real and imaginary parts $\bar{k}_s = k_s + \mathrm{i}m_s$.

In the case of light fluid, a first order development of Eq. (A.1) gives an approximate solution of $\bar{k}_s$. Let rewrite the dispersion equation (A.1) with the dimensional parameters $\epsilon = 2\rho_0/(mk_v)$, $\zeta = k_f/k_v$ and $x = k_s/k_v$, it yields

$$(x^4-1)(\zeta^2 - x^2)^{1/2} = -\mathrm{i}\epsilon \tag{A.2}$$

The first order solution in powers of ϵ is $x = 1 - \mathrm{i}\epsilon/4(\zeta^2-1)^{1/2}$. Finally

$$k_s = \begin{cases} k_v + \frac{\epsilon k_v}{4(1-\zeta^2)^{1/2}} & \text{for } \zeta < 1 \\ k_v & \text{for } \zeta > 1 \end{cases} \tag{A.3}$$

and

$$m_s = \begin{cases} \frac{\eta k_v}{4} & \text{for } \zeta < 1 \\ \frac{\eta k_v}{4} + \frac{\epsilon k_v}{4(\zeta^2-1)^{1/2}} & \text{for } \zeta > 1 \end{cases} \tag{A.4}$$

Remark that $\zeta = c_f/c_v$ where $c_v = (B/m)^{1/4}\sqrt{\omega}$ represents the in vacuo Mach number. For a supersonic structural wave $\zeta > 1$ and for a subsonic wave $\zeta < 1$. We may observe in Eq. (A.4) that when $\zeta < 1$, the structural attenuates under the action of material damping only. But when $\zeta > 1$, the triggering of sound radiation imposes an additional attenuation due to a transfer of energy to the fluid.

Appendix B

We consider the problem of a structural plane wave reflecting on a plate edge [27]. The edge is along the y-axis and the x-axis is inward the plate. The time convention is $\exp(-\mathrm{i}\omega t)$. The structural wavenumber is noted k and is complex-valued.

For a unit incident plane wave with incidence φ with the tangent to the edge (Fig. 3), the deflection is

$$v = \Big[\exp(-\mathrm{i}kx\sin\varphi) + R_s\exp(\mathrm{i}kx\sin\varphi) + R_e\exp(-kx\sqrt{1+\cos^2\varphi})\Big] \times \exp(\mathrm{i}ky\cos\varphi) \tag{B.1}$$

The boundary conditions determine the unknowns R_s and R_e. Three cases are solved. First, for a simply supported edge, the boundary conditions are

$$v(0,y) = \frac{\partial^2 v}{\partial x^2}(0,y) + \nu\frac{\partial^2 v}{\partial y^2}(0,y) = 0 \tag{B.2}$$

By remarking that $\partial_{yy}v = 0$ since $v = 0$ along the y-axis, this leads to the set of linear equations

$$0 = 1 + R_s + R_e, \tag{B.3}$$

$$0 = (1+R_s)\sin^2\varphi - R_e\left[1+\cos^2\varphi\right] \tag{B.4}$$

The solution is $R_s = -1$, $R_e = 0$ given in Eqs. (33), (36).

Second, for a clamped edge, the conditions are

$$v(0,y) = \frac{\partial v}{\partial x}(0,y) = 0, \tag{B.5}$$

that is

$$0 = 1 + R_s + R_e \tag{B.6}$$

$$0 = \mathrm{i}(1-R_s)\sin\varphi + R_e\sqrt{1+\cos^2\varphi} \tag{B.7}$$

The solution is given in Eqs. (34), (37).

Finally, the free edge conditions are

$$\frac{\partial^2 v}{\partial x^2}(0,y)+\nu\frac{\partial^2 v}{\partial y^2}(0,y)=\frac{\partial^3 v}{\partial x^3}(0,y)+(2-\nu)\frac{\partial^3 v}{\partial x\partial y^2}(0,y)=0 \tag{B.8}$$

that is

$$0=(1+R_s)(\sin^2\varphi+\nu\cos^2\varphi)-R_e\left[1+(1-\nu)\cos^2\varphi\right] \tag{B.9}$$

$$0=(1-R_s)\sin\varphi\left[1+(1-\nu)\cos^2\varphi\right]+\mathrm{i}R_e\sqrt{1+\cos\varphi^2}\left[1-(1-\nu)\cos^2\varphi\right] \tag{B.10}$$

The solution is given in Eqs. (35), (38).

References

[1] J.B. Keller, The geometrical theory of diffraction, in: Calculus of Variations and its Applications, McGraw-Hill, New-York, 1958.
[2] J.B. Keller, Geometrical theory of diffraction, J. Opt. Soc. Amer. 52 (2) (1952) 116–130.
[3] G.L. James, GeometricaL Theory of Diffraction for Electromagnetic Waves, IEE Peter Peregrinus Ltd., London, 1976.
[4] J.D. Achenbach, A.K. Gautesen, Geometrical theory of diffraction for three-d elastodynamics, J. Acoust. Soc. Am. 61 (1977) 413–421.
[5] J.D. Achenbach, A.K. Gautesen, H. McMaken, Ray meThods for Waves in Elastic Solids, Pitman, Boston, 1982, chap. 7.
[6] B.D. Seckler, J.B. Keller, Geometrical theory of diffraction in inhomogeneous media, J. Acoust. Soc. Am. 31 (1959) 192–205.
[7] A.D. Pierce, Diffraction of sound around corners and over wide barriers, J. Acoust. Soc. Am. 55 (1974) 941–955.
[8] P. Saha, A.D. Pierce, Geometrical theory of diffraction of an open rectangular box, J. Acoust. Soc. Am. 75 (1984) 46–49.
[9] F. Coulouvrat, Sonic boom in the shadow zone: a geometrical theory of diffraction, J. Acoust. Soc. Am. 111 (2002) 499–599.
[10] E. Reboul, A. Le Bot, J. Perret-Liaudet, Radiative transfer equation for multiple diffraction, J. Acoust. Soc. Am. 118 (2005) 1326–1334.
[11] D.J. Chappell, D. Löchel, N. Sondergaard, G. Tanner, Dynamical energy analysis on mesh grids: a new tool for describing the vibro-acoustics response of complex mechanical structures, Wave Motion 51 (2014) 589–597.
[12] A. Le Bot, E. Reboul, High frequency vibroacoustics: a radiative transfer equation and radiosity based approach, Wave Motion 51 (2014) 598–605.
[13] A. Le Bot, FoundAtion of Statistical Energy Analysis in Vibroacoustics, Oxford University Press, 2015.
[14] N. Tsingos, T. Funkhouser, A. Ngan, I. Carlbom, Modeling acoustics in virtual environments using the uniform theory of diffraction, in: Proceedings of the 28th Annual Conference on Computer Graphics and Interactive Techniques, 2001, pp. 545–552.
[15] D.G. Crighton, The 1988 rayleigh medal lecture: fluid loading–the interaction between sound and vibration, J. Sound Vib. 133 (1989) 1–27.
[16] F. Fahy, P. Gardonio, Sound and Structural Vibration - Radiation, Transmission and Response, Academic Press, 2006.
[17] T.K. Kapoor, L.B. Felsen, Hybrid ray-mode analysis of acoustic scattering from a finite, fluid-loaded plate, Wave motion 22 (1995) 109–131.
[18] L. Cremer, M. Heckl, E.E. Ungar, Structure-borne Sound, Springer-Verlag, 1988.
[19] H.G. Davies, Natural motion of a fluid-loaded semi-infinite membrane, J. Acoust. Soc. Am. 55 (1974) 213–219.
[20] D.G. Crighton, Acoustic edge scattering of elastic surface waves, J. Sound Vib. 22 (1972) 25–32.
[21] D.G. Crighton, D. Innes, The modes, resonances and forced response of elastic structures under heavy fluid loading, Philos. Trans. R. Soc. Lond. A Math. Phys. Eng. Sci. 312 (1984) 295–381.
[22] V. Cotoni, Modélisation de phénomènes vibroacoustiques en moyennes et hautes fréquences par méthode énergétique locale, thesis École centrale de Lyon, France, 2001.
[23] V. Cotoni, A. Le Bot, L. Jezequel, Sound transmission through a plate by an energy flow approach, Acta Acust. United Acust. 88 (2002) 827–836.
[24] M.C. Junger, D. Feit, Sound, Structures and Their Interaction, MIT Press, 1972, p. 167.
[25] V. Cotoni, A. Le Bot, Radiation of plane structures at high frequency using an energy method, Int. J. Acoust. Vibr. 6 (2001) 209–214.
[26] V. Cotoni, A. Le Bot, L. Jezequel, High frequency radiation of l-shaped plates by a local energy flow approach, J. Sound Vib. 250 (2002) 431–444.
[27] K.F. Graff, Wave Motion in Elastic Solids, Dover publications, 1991, p. 245.